Article

pubs.acs.org/Biomac

Shell-Sheddable, pH-Sensitive Supramolecular Nanoparticles Based on Ortho Ester-Modified Cyclodextrin and Adamantyl PEG

Ran Ji, Jing Cheng, Ting Yang, Cheng−Cheng Song, Lei Li, Fu-Sheng Du,* and Zi-Chen Li*

Beijing National Laboratory for Molecular Sciences, Key Laboratory of Polymer Chemistry and Physics of Ministry of Education, College of Chemistry and Molecular Engineering, Peking University, Beijing 100871, China

Supporting Information

ABSTRACT: We report a new type of pH-sensitive supramolecular aggregates which possess a programmable character of sequential dePEGylation and degradation. As a platform of designing and building multifunctional supramolecular nanoparticles, a family of 6-OH ortho ester-modified β-cyclodextrin (β-CD) derivatives have been synthesized via the facile reaction between β-CD and cyclic ketene acetals with different alkyl lengths. These asymmetric acid-labile β-CD derivatives formed amphiphilic supramolecules with adamantane-modified PEG through host−guest interaction in polar solvents such as ethanol. The supramolecules can self-assemble in water to form acid-labile supramolecular aggregates. The results of TEM and light scattering measurements demonstrate that the size and morphology of the aggregates are influenced by the alkyl or PEG length and the host−guest feed ratio. By carefully balancing the alkyl and PEG lengths and adjusting the host−guest ratio, well-dispersed vesicles (50−100 nm) or sphere-like nanoparticles (200−500 nm) were obtained. Zeta potential measurements reveal that these supramolecular aggregates are capable of being surface-functionalized via dynamic host−guest interaction. The supramolecular aggregates were stable at pH 8.4 for at least 12 h as proven by the ^{1}H NMR and LLS measurements. However, rapid dePEGylation occurred at pH 7.4 due to the hydrolysis of the ortho ester linkages locating at the interface, which resulted in aggregation of the dePEGylated hydrophobic inner cores. Upon further decreasing the pH to 6.4, the hydrophobic cores were further degraded due to the acid-accelerated hydrolysis of the ortho esters. The incubation stability of the acid-labile supramolecular aggregates in neutral buffer could be improved by incorporating hydrophobic poly(ε-caprolactone) into the core of the aggregates.

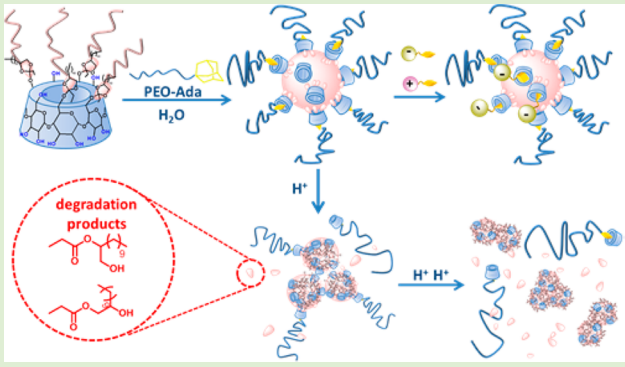

INTRODUCTION

Supramolecules have attracted great attention because of their expansibility in molecular architecture and reversible nature as noncovalent materials.[1−6] Cyclodextrins (CDs), a family of cyclic oligosaccharides exhibiting excellent biocompatibility and versatile host−guest interaction with a wide range of guest molecules, play important roles in both scientific research and application areas as key building components to construct various supramolecules and the relevant materials.[7−9] The CD-based supramolecular nanoparticles or hydrogels have been thoroughly exploited to develop various biomedical materials.[10−16] In addition, CD-containing supramolecules or supramolecular self-assemblies responding to pH,[17] light,[18−21] voltage,[22] enzyme,[23] lectins,[24] or multistimuli[25−27] have been developed, showing potential for intelligent delivery systems. Among them, the pH-sensitive supramolecular systems are promising as the vehicles of nanomedicines due to the numerous pH gradients in human body. While most of the pH-sensitive CD-containing supramolecular systems are based on the switchable host−guest interaction following a pH change,[17,28−31] only limited publications report the supramolecular systems whose pH-sensitivity is due to the acid-cleavable linkages.[32−34]

Polyethylene glycol (PEG) has been widely used to modify proteins,[35] liposomes,[36] polyplexes,[37] and other polymeric nanoparticles,[38] in general, termed as PEGylation, to avoid them being eliminated by the reticulo-endothelial system and prolong their circulation time in blood.[39,40] However, over PEGylation may cause the risk of systemic overexposure of the drug-loaded nanoparticles and hinder their cellular uptake after localizing at the pathological site.[41,42] To solve this "PEG dilemma", scientists have proposed a smart shedding or "dePEGylation" strategy in which the protective PEG or other shielding polymers can be fully or partially removed from the nanoparticle surface upon microenvironmental change at the target sites.[43−45] Various stimuli including pH,[46−48] reduction potential,[49−51] enzyme,[24,52,53] light,[54,55] and so forth, have been applied to trigger the shedding processes, resulting in the changes of morphology or surface property of

Received: May 18, 2014
Revised: July 24, 2014
Published: August 21, 2014

Scheme 1. Functionalizable and PEG-Sheddable Supramolecular Nanoparticles

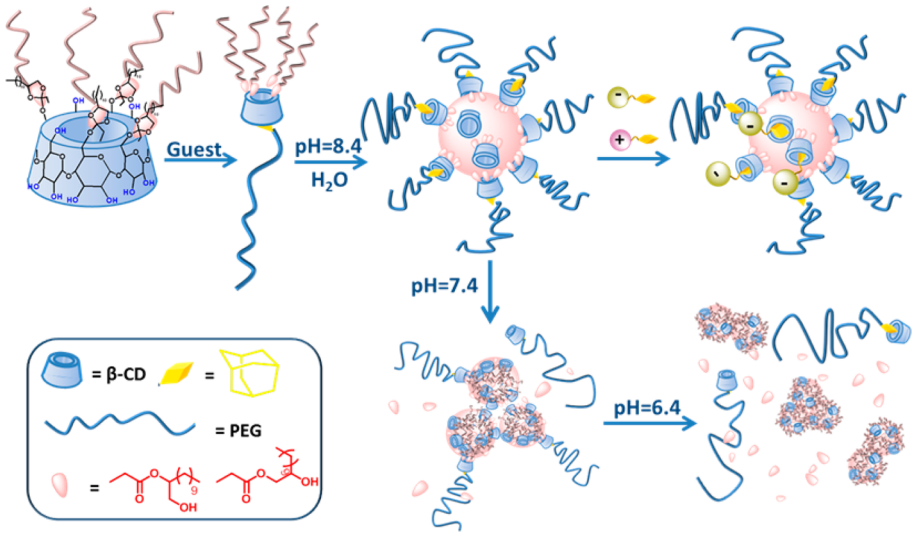

the nanoparticles, or enhancing release rate of the active agents. Furthermore, dual- or multi-stimuli-responsive polymers have attracted a growing interest to construct versatile programmed nanomedicines,[56,57] including the dual pH-sensitive polymeric prodrug with a charge-switching character.[58] However, these programmed systems need generally complicated syntheses or fabrication procedures. Supramolecular chemistry could simplify the molecular design and provide a useful way for the development of programmed nanomedicines.

Ortho ester represents one of the most acid-labile motifs and is widely used as the acid-cleavable linkage in various pH-sensitive delivery systems.[59,60] Recently, we have developed a facile approach to prepare acid-labile polymers with pendent cyclic ortho esters by modifying polyols with highly reactive cyclic ketene acetals (CKA). Primary hydroxyl group is much more active than the secondary one in the reaction.[61] Herein, we have prepared a family of asymmetrically ortho ester-modified β-CD derivatives by the selective reaction of 6-OH of β-CD and CKAs with different alkyl lengths under mild conditions. These acid-labile β-CD derivatives can interact with adamantane-capped PEG to form amphiphilic supramolecules, and some of which can self-assemble into stably dispersed nanoparticles at a mildly basic pH. The empty CD cavities on the surface can be used for further functionalization. Of importance, this type of supramolecular nanoparticles shows a pH-dependent profile of sequential dePEGylation and degradation in the range of physiological pHs, showing potential as carriers of programmed nanomedicines (Scheme 1).

EXPERIMENTAL SECTION

Materials. Triethylamine (TEA), *p*-toluenesulfonic acid (PTSA), D_2O, DCl, 1,2-propanediol, 1,2-octanediol (Aldrich), 1,2-decylanediol (Aldrich), tris(triphenylphosphine) ruthenium(II) dichloride ($(Ph_3P)_3RuCl_2$, Alfa Aesar), 1-adamantanecarbonyl chloride (Ada-CC, Aldrich), and *N*-(1-adamantyl)ethylenediamine (Ada-EA, TCI) were used as received. 1-Adamantanecarboxylic acid (Ada-CA) was prepared by hydrolysis of Ada-CC in 2% NaOH aqueous solution. DMSO-d_6 and $CDCl_3$ (J&K Chemical Ltd.) were dried with CaH_2 and anhydrous Na_2CO_3, respectively, prior to use. DMSO and the other solvents used in cyclodextrin modification were distilled under sodium or CaH_2 prior to use. β-Cyclodextrin was recrystallized from deionized water at 80 °C and dried in vacuum at 40 °C. Methoxypolyethylene glycols (mPEG) with average molecular weights of 750 (J&K Chemical Ltd.), 2000, and 5000 (Aldrich) were used as received. Phosphate buffers (PB) with different pHs (5.5, 6.4, 7.4, and 8.4) were prepared from H_2O, KH_2PO_4, and Na_2HPO_4, and calibrated by a pH meter (Mettler Toledo FE20, Shanghai, China).

Synthesis of Adamantane-End Modified PEGs (Ada-PEGs). Adamantane-end modified PEGs (Ada-PEG 750 as **G1**, Ada-PEG 2000 as **G2**, and Ada-PEG 5000 as **G3**) were synthesized by reaction of the mPEGs with 1-adamantanecarbonyl chloride. The degree of end-functionalization was more than 95% as estimated by the ^{1}H NMR spectra (Figure S1).

Synthesis of Cyclic Ketene Acetals (CKAs). 2-Ethylidene-1,3-dioxane (EDO), 2-ethylidene-4-methyl-1,3-dioxolane (EMD), 2-ethylidene-4-hexyl-1,3-dioxolane (EHD), and 2-ethylidene-4-decyl-1,3-dioxolane (EDD) were synthesized following the published procedure.[61,62] Briefly, diol (0.5 mol), acrolein (0.5 mol), and PTSA (20 mg) were dissolved in toluene (~500 mL) in a flask with a Dean–Stark trap. The solution was refluxed at 120 °C until ~10 mL of water was collected in the trap. Then, the solution was concentrated by rotary evaporation at reduced pressure, followed by addition of CH_2Cl_2 (200 mL). After washing with 30 mL of 1% Na_2CO_3 thrice and 30 mL of saturated NaCl aqueous solution, the organic phase was separated, dried over anhydrous K_2CO_3 overnight, and distilled under reduced pressure, affording vinyl acetal as a colorless liquid. $(Ph_3P)_3RuCl_2$ (50 mg) and vinyl acetal (0.3 mol) were then charged into a 50 mL flask. Under argon atmosphere, the reaction mixture was heated to 125 °C and refluxed for 12 h with magnetic stirring until the isomerization finished. The mixture was distilled under reduced pressure to afford the cyclic ketene acetals. The yields of various CKAs were in the range of 30–60%. All the CKAs and their precursors were characterized by ^{1}H NMR on a Bruker ARX 400 MHz spectrometer (Figures S2–S4).

Synthesis of 6-OH Modified Cyclodextrins. 6-*O*-(2-ethyl-4-methyl-1,3-dioxolan)-2-yl-β-cyclodextrin (EMD-CD) was synthesized through the facile reaction between 2-ethylidene-4-methyl-1,3-dioxolane (EMD) and the primary hydroxyl group (6-OH) of β-cyclodextrin (β-CD). Briefly, β-CD (4.0 g, 3.5 mmol) and PTSA (20 mg) were placed in a round flask and the trace water was removed by azeotropic distillation with 30 mL of anhydrous toluene twice. A total of 20 mL of newly distilled DMSO was added into the flask to completely dissolve the residue. EMD (2.8 g, 24.5 mmol) was predissolved in anhydrous THF for 0.5 h and dropped into the flask. The mixture was stirred at room temperature for additional 1 h followed by adding 0.1 mL of TEA to quench the reaction. The reaction mixture was poured into 150 mL of diethyl ether (with 1% TEA) to afford a white semisolid which was then dissolved in 10 mL of dichloromethane and precipitated in 100 mL of diethyl ether (with 1% TEA) again. The precipitate was isolated by centrifugation and dried in

dx.doi.org/10.1021/bm500711c | *Biomacromolecules* 2014, 15, 3531–3539

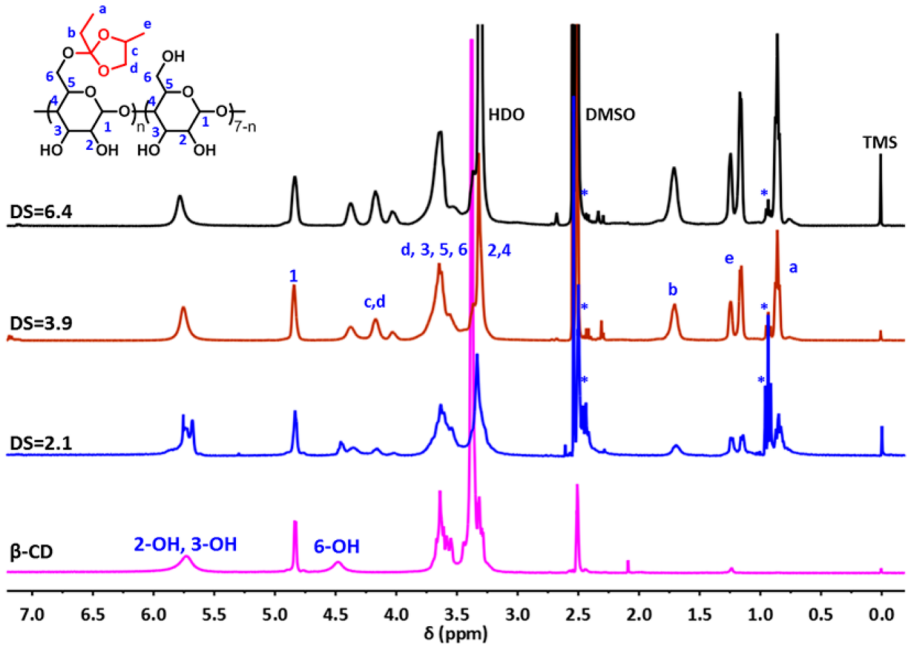

Figure 1. ^{1}H NMR spectra of β-CD and its EMD-modified derivatives in DMSO-d_6. Molar feed ratios of EMD β-CD are 5:1 (DS 2.1), 7:1 (DS 3.9), and 10:1 (DS 6.4), respectively. Degree of substitution (DS), defined as the number of hydroxyl groups reacted with EMD per CD molecule, is determined by comparing the intensity of peak b and peak 1. The asterisk denotes the proton signals of TEA.

vacuo, affording a white powder in 80% yield. The other CKA-modified β-CDs at 6-OH, 6-*O*-(2-ethyl-1,3-dioxan)-2-yl-β-CD (EDO-CD), 6-*O*-(2-ethyl-4-hexyl-1,3-dioxolan)-2-yl-β-CD (EHD-CD), and 6-*O*-(2-ethyl-4-decyl-1,3-dioxolan)-2-yl-β-CD (EDD-CD) were synthesized in a similar way (yields ranging from 40 to 65%). All the CKA-modified CDs were characterized by ^{1}H NMR spectra (Figures 1, S6, and S7).

Self-Assembly of Host–Guest Complex. A thin film hydration method was applied to get dispersions of the acid-labile supramolecular self-assemblies. Take the host–guest system of EDD-CD and **G2** as an example. EDD-CD (9.9 mg, 4.7 μmol) and **G2** (10 mg, 4.7 μmol) were dissolved in ethanol in a flask and the solution was equilibrated for 0.5 h at 40 °C. Then, the solvent was removed by rotary evaporation at reduced pressure to get a transparent film at the bottom of the flask. Phosphate buffer (pH = 8.4, 10 mM, 10 mL) was added into the flask which was ultrasonicated for 0.5 h to afford a transparent dispersion with a final aggregation concentration of 2.0 mg/mL. The other H-G supramolecular aggregates were prepared by the same protocol unless otherwise mentioned. After preparation, the dispersions were quickly frozen in liquid nitrogen and stored at −20 °C, affording stock dispersions with an aggregate concentration of 2.0 mg/mL. For **H3G3**-1.0, the aggregate concentration was 3.5 mg/mL. The stock dispersions were unfrozen by ultrasonication at 20 °C for ∼5 min prior to light scattering and TEM measurements. The freezing–unfreezing process does not influence the size and morphology of the supramolecular aggregates.

Laser Light Scattering (LLS) Measurements. The unfrozen stock dispersion was diluted to 0.2 mg/mL of the aggregate concentration by adding PB (pH = 8.4, 10 mM). After incubation for 2 h at room temperature, the diluted dispersion was filtered into a dust-free vial through a Millipore 0.45 μm PVDF membrane prior to LLS measurement. Both static light scattering (SLS) and dynamic light scattering (DLS) measurements over a scattering angular range of 20–150° were carried out on a commercialized equipment (BI-200SM Goniometer, Holtsville, NY). A 100 mW solid state laser (GXC-III, CNI, Changchun, China) operating at 532 nm was used as the light source. A BI-TurboCo Digital correlator (Brookhaven Inc.) was used to collect and process the data. The root mean square radius of gyration (R_g) was obtained by the following equations:

$$\frac{HC}{R_{vv}(\theta)} = \frac{1}{M_w}\left[1 + \frac{1}{3}R_g^2 q^2\right] + 2A_2C$$

$$H = \frac{4\pi^2 n^2 \left(\frac{dn}{dc}\right)^2}{N_A \lambda^4}, \quad q = \frac{4\pi n}{\lambda}\sin\left(\frac{\theta}{2}\right)$$

where the Rayleigh ratio $R_{vv}(\theta)$ was measured as the angular dependence of the excess absolute time-averaged scattered intensity in SLS, and N_A, n, dn/dc, λ, and θ was the Avogadro's number, the solvent refractive index, the specific refractive index increment, the wavelength of light in vacuo, and the scattering angle, respectively. The hydrodynamic radius R_h was calculated by using the Stokes–Einstein equation $D = k_BT/6\pi\eta R_h$, where D was obtained by extrapolating Γ/q^2 to zero angle. Laplace inversion program, CONTIN, was used to obtain Γ at different angles by normalization of the line width distribution $G(\Gamma)$ obtained from DLS measurements.

Zeta Potential Measurements. Zeta potentials of the aggregates were analyzed on a Zeta PALS analyzer (Brookhaven Instruments Corp.) equipped with a temperature controller and a 35 mW He–Ne solid state laser (λ = 660 nm, detection angle: 90°). The data were measured in triplicate. The **H3G2** supramolecular aggregates (0.2 mg/mL) were prepared following the same procedure as for the LLS measurements. To 1.0 mL of the **H3G2** supramolecular dispersion, 10 μL of Ada-EA or Ada-CC (10 mg/mL in 10 mM PB) was added. The mixture was vortexed for 30 s prior to the measurement. The molar ratio of Ada-EA or Ada-CC to the host was 10:1.

Transmission Electron Microscopy (TEM) and Freeze-Fracture TEM. The supramolecular aggregates used for the preparation of TEM specimens were prepared following the same procedure as for the LLS measurements, with an aggregate concentration of 0.2 mg/mL. The TEM specimen was prepared by dropping 10 μL of dispersion on one piece of copper mesh. After 60 s, most of the liquid was removed by blotting with a filter paper, and the remnant dispersion on the mesh was dried at room temperature for an additional 15 min. Then, 5 μL of phosphotungstic acid aqueous solution (1%, pH = 7.4) was dropped on the copper mesh with aggregates to enhance contrast. After 90 s, most of the staining liquor was removed by blotting with a filter paper, the mesh was dried at room temperature for 12 h before TEM observation on an equipment (JEOL JEM-100CXII) with an acceleration voltage of 100 kV.

dx.doi.org/10.1021/bm500711c | *Biomacromolecules* 2014, 15, 3531–3539

For FF-TEM, the aggregates with a higher concentration (1.0 mg/mL) were prepared in water (with ~1% TEA) following the aforementioned procedure. The aggregate dispersion was dropped on a piece of copper mesh, covered quickly with another copper mesh, and frozen quickly. A freeze-fracture apparatus (Balzers BAF400, Germany) was used to fracture and replicate the sample at −140 °C. After Pt/C was deposited on the sample fracture surface, the organic part was dissolved by acetone. The Pt/C replica was reloaded on a fresh copper mesh and observed by the aforementioned TEM equipment.

pH-Responsive DePEGylation and Degradation of the Aggregates. Hydrolysis of the ortho ester linkage in the supramolecular aggregates was estimated directly by ^{1}H NMR measurement. The dispersion of **H3G2**-0.8 supramolecular aggregates in 1.0 mM PB (pH = 8.4, 2.0 mg/mL) was prepared by the film hydration protocol. After incubation at 37 °C for 6 h, 2.5 mL of the dispersion was taken out and quickly frozen in liquid nitrogen, and used as the sample for 0 min. The remained dispersion was divided into three flask (50 mL/flask) and stirred magnetically. The pH of the dispersion was adjusted by adding ~5 mL of concentrated PB (0.1 M, pH = 6.4, 7.4, and 8.4, respectively). At specific time point, 2.5 mL of the dispersion was taken out, quenched quickly by adding one drop of TEA, and frozen in liquid nitrogen. After lyophilization, 0.5 mL of DMSO-d_6 was added into each sample to thoroughly dissolve the organic compounds. The insoluble phosphate salt was removed by centrifugation, and the hydrolysis products were analyzed by ^{1}H NMR on the Bruker ARX 400 MHz spectrometer (Figure S13).

The pH-responsive dePEGylation of the **H3G2**-0.8 supramolecular aggregates was also monitored by LLS. Briefly, 2 mL of the **H3G2**-0.8 dispersion (0.2 mg/mL) in PB (1.0 mM, pH = 8.4) was filtered into a dust-free vial through a Millipore 0.45 μm PVDF membrane. The dispersion was measured on the aforementioned LLS equipment, and the obtained data were used for 0 min time point. Then, 200 μL of PB (0.1 M, pH = 7.4 or 8.4) was added into the dispersion, which was quickly vortexed for 30 s and measured at different times with a scattering angle of 90° at 37 °C.

For the hydrophobically modified supramolecular aggregates, that is, the mixed aggregates of **H3G3**-1.0 with poly(ε-caprolactone), a dialysis protocol was used. Briefly, **H3** (2.1 mg, 1.0 μmol) and **G3** (5.0 mg, 1.0 μmol) were dissolved in 1 mL of ethanol and equilibrated at 40 °C for 0.5 h. PCL (M_n = 5 kDa, 2.0 mg, 0.4 μmol) was dissolved in 1 mL of ethanol at 40 °C. These two solutions were mixed and equilibrated for an additional 1 h at 40 °C, followed by quickly adding 20 mL of PB (pH = 8.4, 1.0 mM). The mixture was ultrasonicated for 15 min and incubated at 40 °C for 4 h and dialyzed against PB (pH = 8.4, 1.0 mM) for an additional 24 h at 40 °C (MWCO:1 kDa) to afford **H3G3**-1.0-PCL aggregates with a **H3** concentration of 1.0 mg/mL and a PCL/**H3** molar ratio of 0.4. The dispersion was diluted to a **H3** concentration of 0.1 mg/mL by the addition of PB (pH = 8.4, 1.0 mM) and filtered through a Millipore 0.45 μm PVDF membrane. This diluted dispersion was used to evaluate the stability of the aggregates at different pHs (10 mM PB, pH = 7.4, 6.4 or 5.5). The diameter of the aggregates and scattered intensity of the dispersion were measured on the Zeta PALS analyzer (Brookhaven Instruments Corp.) and the data were obtained in triplicate.

RESULTS AND DISCUSSION

Click-Like Reaction between CKA and CD. The reaction between CKAs and the hydroxyl groups of alcohols or polyols can be recognized as a "click" reaction due to its universality, high efficiency, and facile reaction condition.[61,63−65] In addition, the less sterically hindered primary hydroxyl groups are much more active than the secondary ones when they react with CKA.[61,63−65] In order to reveal if there is a difference between the reactivity of the primary hydroxyl group (6-OH) and the secondary hydroxyl groups (2-OH and 3-OH) of cyclodextrins toward CKA, β-CD was applied to react with EMD at different feed ratio at 20 °C, and the reaction products (EMD-CDs) were characterized by ^{1}H NMR spectra (Figure 1). With increasing the molar feed ratio of EMD to hydroxyl groups of β-CD from 5:1 to 10:1, the proton signals of 6-OH at ~4.5 ppm gradually disappeared, while the signals of 2-OH and 3-OH at ~5.7 ppm remained almost constant. Meanwhile, the proton signals assigned to the ortho ester groups (peaks a−e) became gradually stronger. By comparing the intensities of peak b and peak 1, which is assigned to the **C1** proton of the CD ring, degree of substitution (DS) of the hydroxyl groups (by ortho ester groups) can be determined and the results are summarized in Table 1. It is seen that the DS can be tuned in the range of ~2−6.4 by simply changing the molar feed ratio of EMD to β-CD. However, with further increasing the feed ratio up to 21:1, the DS did not change significantly (run 4 vs run 3 in Table 1). These results indicate that EMD selectively react with the primary 6-OH of β-CD but not the secondary 2-OH or 3-OH under the experimental conditions, which may be ascribed to the intramolecular hydrogen bonding between the 2-OH and 3-OH of the adjacent glucose units.[66]

Table 1. Reaction Condition and Results of CKAs and β-CDs

run	CKA	temperature (°C)	feed ratio[a] (CKA/OH)	DS[b]
1	EMD	20	5:1	2.1
2	EMD	20	7:1	3.9
3	EMD	20	10:1	6.4
4	EMD	20	21:1	6.1
5	EMD	40	21:1	19.5
6	EDO	20	21:1	6.5
7	EDO	40	21:1	15.2
8	EHD	20	8:1	4.3
9	EDD	20	8:1	4.1

[a]Molar feed ratio of CKA to hydroxyl groups of β-CD. [b]Degree of substitution (DS) of hydroxyl groups of β-CD by ortho ester groups estimated by ^{1}H NMR spectra.

When EMD reacted with β-CD at 40 °C with a large feed ratio (21:1), both primary (6-OH) and secondary (2- and 3-OH) hydroxyl groups were modified by the ortho ester groups. As shown in Figure S5, the original narrow peak at ~4.8 ppm that is assigned to the **C1** proton of the intact β-CD or the 6-OH substituted β-CD derivatives shifted downfield to ~4.9 ppm and became broader, which is consistent with substitution at 2-OH or 3-OH of β-CD.[67] The DS reached ~20, as estimated by comparing the signal intensities of the **C1** proton and proton b at ~1.8 ppm (run 5 in Table 1). When another six-membered CKA (EDO) was used to react with β-CD at a feed ratio of 21:1, the similar phenomenon was observed with a DS of 6.5 at 20 °C and a much higher DS (~15) at 40 °C (Figure S6 and Table 1).

These results are understandable because increasing temperature would disrupt, at least weaken, the hydrogen bonding between 2-OH and 3-OH, and make them reactive to the CKAs. On the whole, β-CD can be easily modified by CKA to afford acid-labile derivatives with cyclic ortho ester groups. The DS can be tuned by simply changing the feed ratio or reaction temperature. Asymmetrically ortho ester-modified β-CD derivatives can be easily prepared at a relatively low temperature (Scheme 2). On this basis, two CKAs with longer alkyl chains (**EHD** and **EDD**) were applied to modify β-CD, affording additional two acid-labile β-CD derivatives (EHD-CD

Scheme 2. Reaction between CKAs and β-CDs

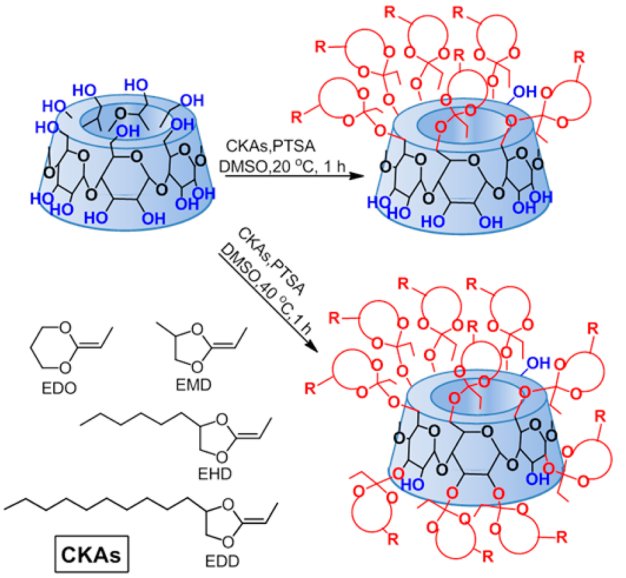

and EDD-CD) with a DS in the range of 4−4.5 (Figure S7 and Table 1).

Self-Assembly of Supramolecules. All of the CKA-CDs except run 1 shown in Table 1 are not soluble in water because of their hydrophobicity and cannot form stably dispersed nanoparticles in aqueous media directly by themselves. However, they are able to form amphiphilic supramolecules with adamatane-modified PEG (Ada-PEG) through host−guest interaction between the adamantyl group and CD ring. These acid-labile supramolecules may self-assemble into nanoparticles of various morphologies and sizes. Here, we selected three asymmetrically modified CKA-CDs with different alkyl chain lengths as the hosts (**H1**, **H2**, and **H3**) and three Ada-PEG of different PEG lengths as the guest molecules (**G1**, **G2**, and **G3**) and studied the aggregation profiles of the supramolecules formed by various H-G pairs (Scheme 3). In order to find an

Scheme 3. Host and Guest Molecules Used in the Supramolecular Self-Assembly

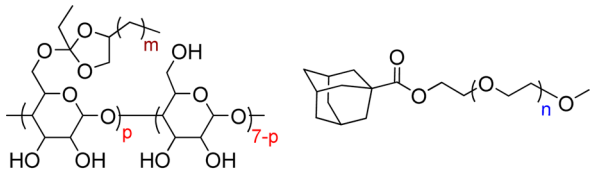

H1: EMD-CD, m = 0, p = 6.1
H2: EHD-CD, m = 5, p = 4.3
H3: EDD-CD, m = 9, p = 4.1

G1: n = 16
G2: n = 44
G3: n = 113

appropriate method to get stably dispersed supramolecular nanoparticles, **H3**-**G2** pair in a molar ratio of 1:1 was first studied by using the film hydration protocol. When THF or $CHCl_3$ was used as a solvent to prepare supramolecular thin film, it is difficult to obtain well-dispersed nanoparticles upon ultrasonication in phosphate buffer. However, if supramolecular thin film was prepared by using ethanol or methanol as organic solvent, hydration of the film under ultrasonication afforded well dispersed supramolecular nanoparticles. These results can be attributed to the difference in polarity of the used solvents. In the less polar THF or $CHCl_3$, **H3** and **G2** could hardly form an inclusion complex; therefore, there were little preformed amphiphilic supramolecules in the thin film. In ethanol or methanol with a strong polarity, the host−guest interaction between **H3** and **G2** is much stronger than in THF or $CHCl_3$, which favors the preformation of the amphiphilic supramolecules in the film.[68,69]

By using the same procedure with ethanol as the organic solvent, the aggregation behaviors of the other H-G pairs in a molar ratio of 1:1 were investigated and the results are shown in Table S1. Both alkyl length of the hosts and PEG length of the guests influence the aggregation of the H-G supramolecules. In case of **G1**, all three of the H-G pairs formed macroscopic precipitates probably due to the short PEG chain, which is not long enough to effectively stabilize the supramolecular aggregates. For the longer **G2** and **G3**, the stably dispersed nanoparticles were only formed by pairs of **H2G2**, **H3G2**, and **H3G3**; the other three pairs did not show obvious aggregation due to the high degree of hydrophilic−lipophilic balance. **H3G2** supramolecular nanoparticles have a vesicular morphology with a small diameter (∼50−80 nm), while **H3G3** formed sphere-like nanoparticles with a diameter of ∼100−220 nm (Figure 2 and Table 2). **H2G2** supramolecular aggregates may possess a loose structure, as indicated by the large diameter (∼350−550 nm) and R_g/R_h (∼1.8), which limits the application of the aggregates as carriers for nanomedicine (Figure S8 and Table S1).

Besides the alkyl or PEG chain length, the ratio of host to guest exerts a significant effect on the size and morphology of the H-G supramolecular aggregates (Figure 2 and Table 2). The aggregates gradually evolved from small vesicles to large solid-like nanospheres as the **H3**/**G2** molar ratio increased. With increasing the **H3**/**G2** ratio from 1:1 to 1:0.9, both size of the vesicles and thickness of the vesicular membrane increased, implying that more **H3** molecules were incorporated into the membrane. Further increase in **H3**/**G2** ratio resulted in the disappearance of the supramolecular vesicles, and instead the formation of sphere-like loose aggregates at the ratio of 1:0.8 and more compact solid-like particles at the ratio of 1:0.7, respectively. The morphologies of **H3G2** aggregates were also supported by their different loading capacities for water-soluble model compound, 6-carboxyfluorescein (6-CF; Table S3). While **H3G2**-1.0 and **H3G2**-0.9 vesicles were able to effectively load 6-CF in their hydrophilic interior, **H3G2**-0.7 nanoparticle showed little capability of loading 6-CF due to the solid-like inner structure. The loading capacity of H3G2−0.8 aggregate was smaller than that of the **H3G2**-1.0 or **H3G2**-0.9 vesicle but much larger than that of the **H3G2**-0.7 nanoparticle, implying the loose structure of **H3G2**-0.8 aggregate. These results are illustrated in Scheme 4. In the case of **H3G3** supramolecular aggregates, the particle size decreased with increasing **H3**/**G3** molar ratio from 1:1 to 1:0.7, no vesicular structure was formed (Table S2).

Surface Modification of the Supramolecular Aggregates. To demonstrate whether the surface CD cavities can be used for further functionalization of the supramolecular aggregates, Ada-EA and Ada-CC as the charged model guests were added into the dispersions of **H3G2** aggregates with different **H3**/**G2** feed ratios, and zeta potentials of the aggregates were measured at different times. As shown in Figure 3, in the absence of the charged guests, all the aggregates have similar zeta potentials of ∼-10 mV. After 5 min of adding 10-fold of Ada-EA (compared to **H3**), zeta potential of the aggregates increased gradually from −8.6 mV for **H3G2**-1.0 to

dx.doi.org/10.1021/bm500711c | *Biomacromolecules* 2014, 15, 3531−3539

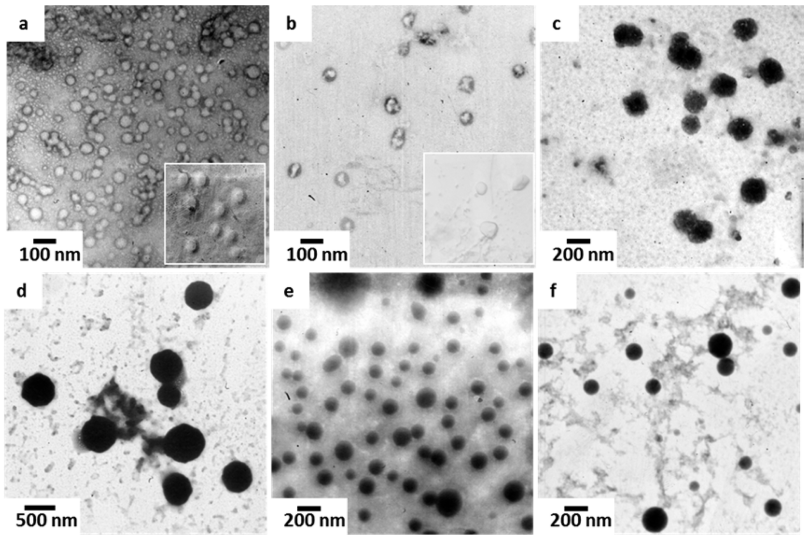

Figure 2. TEM images of the H-G Supramolecular aggregates. (a) **H3G2**-1.0 vesicles (inset: FF-TEM image), (b) **H3G2**-0.9 vesicles, (c) **H3G2**-0.8 nanoparticles, (d) **H3G2**-0.7 nanoparticles, (e) **H3G3**-1.0 nanoparticles, and (f) **H3G3**-1.0-PCL nanoparticles. For **H3G2** supramolecules, concentration of the aggregates was 0.2 mg/mL; for **H3G3** systems, concentration of **H3** in the aggregates was 0.1 mg/mL. pH = 8.4 (1.0 mM PB); stained with phosphotungstic acid (1%, pH = 7.4).

Table 2. Characterization of H3G2 and H3G3 Aggregates

aggregate	n_{host}/n_{guest} [a]	R [b] (nm)	R_g [c] (nm)	R_h [c] (nm)	R_g/R_h	morphology
H3G2-1.0	1.0/1.0	20−35	48	44	1.09	vesicle
H3G2-0.9	1.0/0.9	30−60	73	72	1.01	vesicle
H3G2-0.8	1.0/0.8	90−110	125	127	0.99	nanoparticle
H3G2-0.7	1.0/0.7	150−250	278	322	0.86	nanoparticle
H3G3-1.0	1.0/1.0	50−110	118[d]	136[d]	0.87[d]	nanoparticle
H3G3-1.0-PCL	1.0/1.0	30−120	79	115	0.69	nanoparticle

[a]Molar ratio of host to guest. [b]Average radius measured by TEM. [c]Average hydrodynamic radius (R_h) and the radius of gyration (R_g) measured by LLS, 0.2 mg/mL in phosphate buffer (pH = 8.4, 10 mM), 37 °C. [d]Averaged data of two measurements.

Scheme 4. Morphological Change of the H3G2 Supramolecular Aggregates with Increasing the H/G Molar Ratio

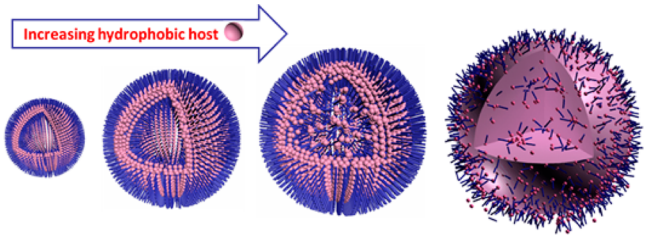

12.5 mV for **H3G2**-0.7. By contrast, when the negatively charged Ada-CC (10-fold to **H3**) was added, zeta potential of the aggregates decreased gradually from −12.4 mV for **H3G2**-1.0 to −35.3 mV for **H3G2**-0.7. For the same aggregate, for example, **H3G2**-0.7, adding Ada-EA increased zeta potential from −9 to 12.5 mV, while the addition of Ada-CC made zeta potential dropped from −9 to −36 mV. These results indicate that the supramolecular aggregates are capable of being functionalized via host−guest interaction; the degree of functionalization increases with increasing the **H3**/**G2** feed ratio because there would be more empty cavities at a relatively high **H3**/**G2** ratio. Interestingly, when the mixture of **H3G2** aggregates and Ada-CC was incubated for a longer time (1 h), the difference in zeta potential of the aggregates diminished and all the four samples showed the similar zeta potentials (−20−25 mV). This phenomenon can be attributed to the dynamic mechanism of the host−guest interaction.

pH-Responsive DePEGylation and Degradation of the Aggregates. The effect of pH on **H3G2**-0.8 supramolecular aggregates with incubation time was first studied by using LLS. As shown in Figure 4a, both R_h of the aggregates and scattered intensity of the dispersion did not change obviously in 12 h at pH 8.4, indicating that the aggregates were stable. By contrast, at pH 7.4, both R_h and intensity increased greatly from beginning of the incubation, and the apparent R_h reached a value larger than 1000 nm after 150 min. TEM images reveal that large clusters composed of smaller spherical nanoparticles adhered together were formed after incubation for 12 h at pH 7.4 (Figure S11). The hydrolysis behaviors of the aggregates were further investigated by ^{1}H NMR spectroscopy at different pHs (Figure S13). The kinetic curves of hydrolysis of the ortho ester calculated from the ^{1}H NMR spectra are shown in Figure 4b. At pH 8.4, hydrolysis rate of the ortho ester was very slow with a hydrolysis degree less than 5% in 10 h. At pH 7.4, the ortho ester hydrolyzed much faster at the initial stage, with a hydrolysis degree of ∼10% within 1 h; however, the kinetic curve almost leveled off in the following ∼9 h. When pH of the buffer decreased to 6.4, the kinetic curve became S-shaped. At the initial stage, the ortho ester hydrolyzed faster than at pH 7.4, reaching a hydrolysis degree of ∼11% in 30 min. After a period with a very slow hydrolysis rate (30−300 min), the hydrolysis rate of the ortho ester increased again.

dx.doi.org/10.1021/bm500711c | *Biomacromolecules* 2014, 15, 3531−3539

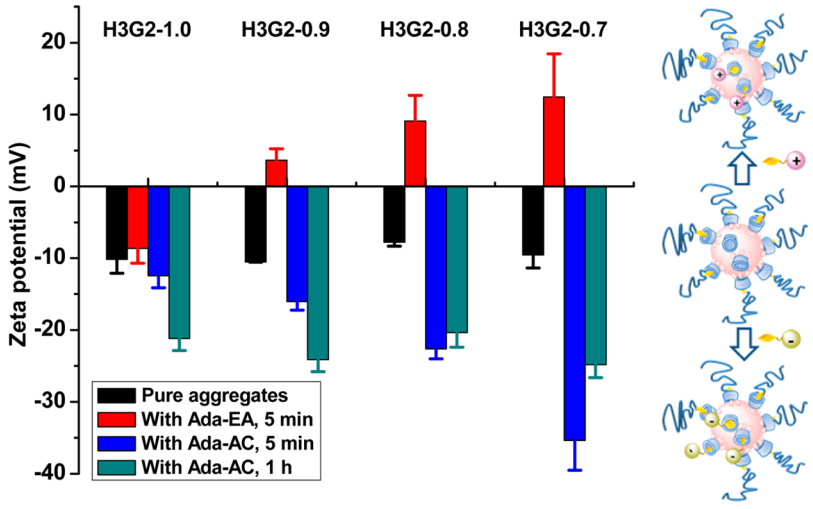

Figure 3. Zeta potentials of the supramolecular aggregates in the absence or presence of Ada-EA or Ada-AC. Concentration of aggregate, 0.2 mg/mL; concentration of Ada-EA or Ada-AC, 0.1 mg/mL; pH = 8.4 (10 mM PB).

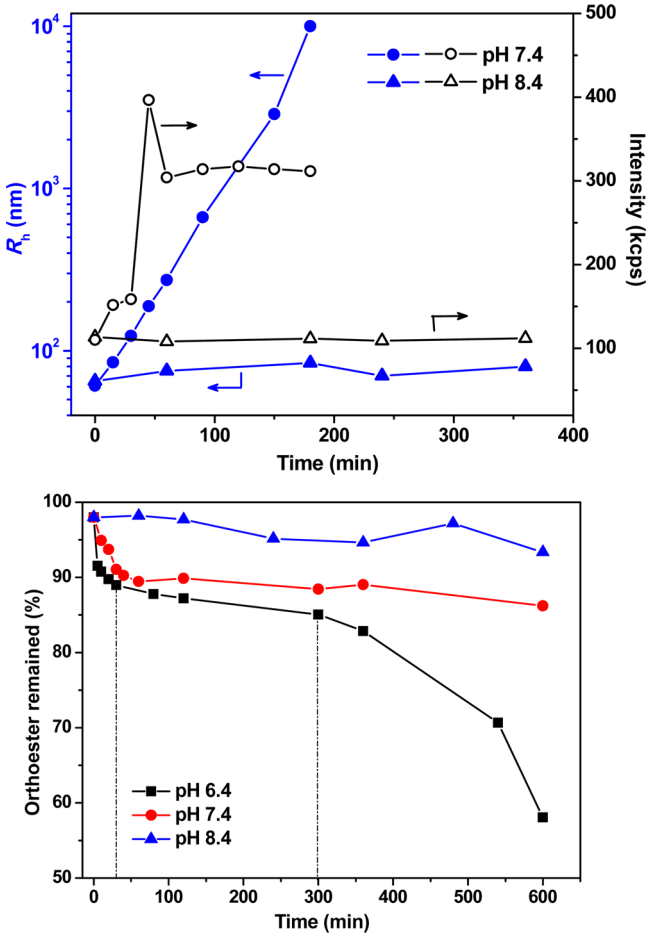

Figure 4. (a) Scattered light intensity and hydrodynamic radius (R_h) of **H3G2**-0.8 aggregates at different incubation time at pH 7.4 and 8.4, respectively: detected angle, 90°; concentration of aggregates, 0.2 mg/mL. (b) Remaining ortho ester (percentage) in the aggregates at different pH and incubation time: PB concentration, 10 mM; 37 °C.

These results can be rationally demonstrated in Scheme 5. As we reported previously, the ortho ester linkage used in this work is relatively stable in the weakly basic phosphate buffer (pH = 8.4) but extremely labile to a mildly acidic condition, and even unstable in neutral aqueous buffer.[61] In addition, the ortho ester linkages in the supramolecular aggregates can be divided roughly into two types; most of them are inside the hydrophobic core and the others locate at or near the relatively hydrophilic interface between the core and the PEG shell. The incubation stability of the aggregates at pH 8.4 is guaranteed by the PEG shell due to the relative stability of ortho ester. At pH 7.4, the ortho ester linkages locating at the interface quickly hydrolyzed, causing dePEGylation and the subsequent aggregation of the dePEGylated hydrophobic inner cores. The remained ortho esters (~90%) inside the cores (or their clusters) would be much stable due to the hydrophobic microenvironment and hydrolyzed very slowly at neutral pH. It is well-known that, besides pH and molecular structure, hydrolysis kinetics of ortho ester is also greatly influenced by the hydrophilic/hydrophobic balance of microenvironment.[70,71] Upon further decreasing the pH to 6.4, the hydrophobic cores or their clusters can be further degraded due to the acid-accelerated hydrolysis of the ortho esters. Using nile red (NR) as a hydrophobic fluorescent probe, we studied the pH-dependent releasing behaviors of NR from **H3G2**-0.8 nanoparticles (Figure S14). The normalized intensity of NR did not significantly decreased (<10% in 24 h) at pH 8.4, which indicates that the nanoparticles were stable. With decreasing pH, the intensity decreased greatly. The lower the pH, the faster release of NR.

As an ideal pH-sensitive programmable delivery system targeting the remote tumor tissues, the nanoparticles should be stable enough at pH 7.4 to ensure a long circulation in blood. Unfortunately, as aforementioned, **H3G2**-0.8 nanoparticles were unstable even at pH 7.4. In the case of **H3G3**-1.0 nanoparticles, which contain the longer PEG chains as the hydrophilic shell, the incubation stability was still poor, with only a slight improvement as compared to the **H3G2**-0.8 nanoparticles (Figure S15). In order to further improve the stability at pH 7.4, the mixed supramolecular nanoparticles were prepared by incorporating hydrophobic poly(ε-caprolactone) (PCL) into the core of the **H3G3**-1.0 aggregates. As shown in Figure 5, the incubation stability of the mixed nanoparticles (**H3G3**-1.0-PCL) in neutral buffer was greatly improved, with only a little decrease in the scattered intensity and a negligible change in size of the nanoparticles in 16 h. At

dx.doi.org/10.1021/bm500711c | *Biomacromolecules* 2014, 15, 3531−3539

Scheme 5. pH-Responsive Sequential DePEGylation and Degradation of the Supramolecular Aggregates

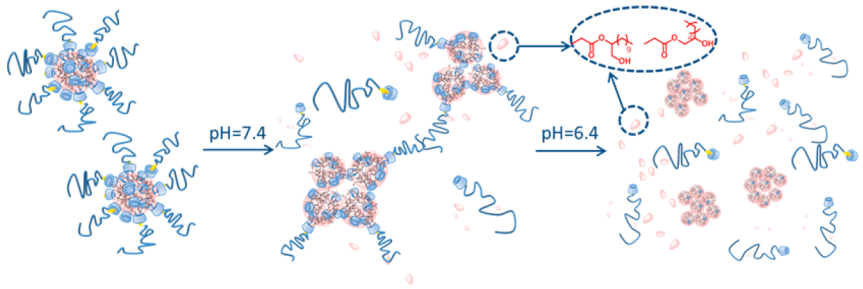

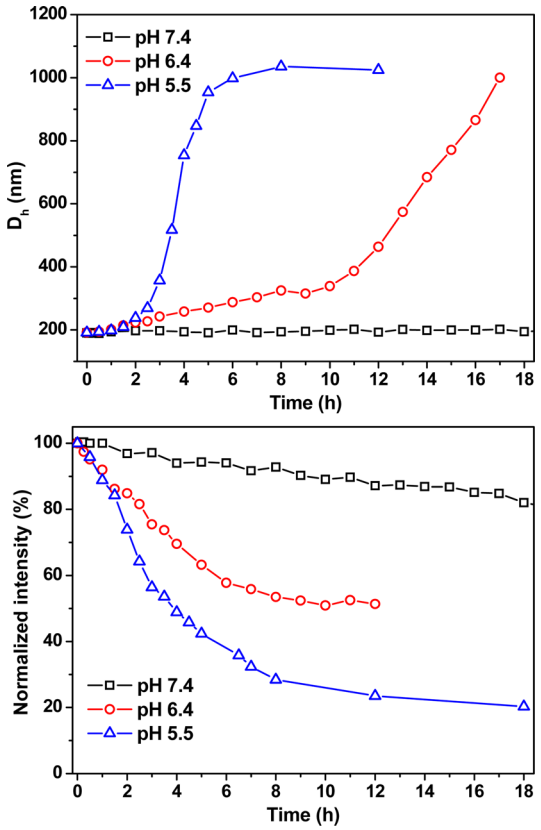

Figure 5. Changes in (a) diameter and (b) scattered intensity of the **H3G3**-1.0-PCL supramolecular aggregates at different incubation times and various pHs: detected angle, 90°; concentration of **H3**, 0.1 mg/mL; PCL/**H3** molar ratio, 0.4; PB (10 mM); 37 °C.

the lower pHs, the size of the nanoparticles increased and the scattered intensity of the dispersion decreased gradually due to the acid-triggered dePEGylation and the subsequent formation of hydrophobic clusters that easily precipitated. The lower the pH, the faster the dePEGylation occurred.

CONCLUSIONS

β-CD can be easily modified by CKA to afford acid-labile *β*-CD derivatives with cyclic ortho ester groups. The DS can be manipulated simply by changing the feed ratio or reaction temperature. A family of 6-OH ortho ester-modified *β*-CD derivatives with different alkyl lengths have been easily prepared at a relatively low temperature. The asymmetrically modified *β*-CD derivatives have the ability to form acid-labile supramolecules with Ada-PEG in the polar solvents. The supramolecules with appropriate alkyl and PEG lengths self-assemble into well-dispersed aggregates, the size, and morphology of which are influenced by the host−guest feed ratio, changing from smaller vesicles to larger solid-like spherical nanoparticles. These supramolecular aggregates are stable at pH 8.4 but show a pH-dependent profile of the sequential dePEGylation and degradation. Ease of fabrication, capability of further functionalization via kinetic host−guest interaction, and pH-sensitivity enables this type of supramolecular aggregate, promising candidates for programmable drug delivery systems targeting the diseased sites with tiny pH gradients.

ASSOCIATED CONTENT

Supporting Information

^{1}H NMR spectra of the guest molecules (**G1**−**G3**), CKAs, and their precursors; more CKA-modified CD derivatives, and the aggregates **H3G2**-0.8 incubated at different pH and time; more TEM images and LLS results. This material is available free of charge via the Internet at http://pubs.acs.org.

AUTHOR INFORMATION

Corresponding Authors

*Phone: +86-10-62757155. Fax: +86-10-62751708. E-mail: fsdu@pku.edu.cn.

*Phone: +86-10-62755543. Fax: +86-10-62751708. E-mail: zcli@pku.edu.cn.

Notes

The authors declare no competing financial interest.

ACKNOWLEDGMENTS

This work was financially supported by the National Natural Science Foundation of China (21174002 and 21090351) and the National Science Fund for Distinguished Young Scholars of China (21225416).

REFERENCES

(1) Wenz, G. *Angew. Chem., Int. Ed.* **1994**, *33*, 803−822.
(2) Sijbesma, R. P.; Beijer, F. H.; Brunsveld, L.; Folmer, B. J. B.; Hirschberg, J.; Lange, R. F. M.; Lowe, J. K. L.; Meijer, E. W. *Science* **1997**, *278*, 1601−1604.
(3) Harada, A. *Acc. Chem. Res.* **2001**, *34*, 456−464.
(4) Beck, J. B.; Rowan, S. J. *J. Am. Chem. Soc.* **2003**, *125*, 13922−13923.
(5) Harada, A.; Takashima, Y.; Yamaguchi, H. *Chem. Soc. Rev.* **2009**, *38*, 875−882.
(6) Zhang, X.; Wang, C. *Chem. Soc. Rev.* **2011**, *40*, 94−101.
(7) Davis, M. E.; Brewster, M. E. *Nat. Rev. Drug Discovery* **2004**, *3*, 1023−1035.
(8) Chen, G.; Jiang, M. *Chem. Soc. Rev.* **2011**, *40*, 2254−2266.
(9) Wang, L.; Li, L. L.; Fan, Y. S.; Wang, H. *Adv. Mater.* **2013**, *25*, 3888−3898.

(10) Davis, M. E.; Zuckerman, J. E.; Choi, C. H. J.; Seligson, D.; Tolcher, A.; Alabi, C. A.; Yen, Y.; Heidel, J. D.; Ribas, A. *Nature* **2010**, *464*, 1067−1070.
(11) Davis, M. E. *Mol. Pharmaceutics* **2009**, *6*, 659−668.
(12) Li, J.; Loh, X. J. *Adv. Drug Delivery Rev.* **2008**, *60*, 1000−1017.
(13) Moya-Ortega, M. D.; Alvarez-Lorenzo, C.; Concheiro, A.; Loftsson, T. *Int. J. Pharm.* **2012**, *428*, 152−163.
(14) Zhang, J.; Ma, P. X. *Adv. Drug Delivery Rev.* **2013**, *65*, 1215−1233.
(15) Zhang, J.; Jia, Y.; Li, X.; Hu, Y.; Li, X. *Adv. Mater.* **2011**, *23*, 3035−3040.
(16) Fan, H.; Hu, Q.-D.; Xu, F.-J.; Liang, W.-Q.; Tang, G.-P.; Yang, W.-T. *Biomaterials* **2012**, *33*, 1428−1436.
(17) Park, C.; Oh, K.; Lee, S. C.; Kim, C. *Angew. Chem., Int. Ed.* **2007**, *46*, 1455−1457.
(18) Yan, Q.; Xin, Y.; Zhou, R.; Yin, Y.; Yuan, J. *Chem. Commun.* **2011**, *47*, 9594−9596.
(19) Liu, Y.; Yu, C.; Jin, H.; Jiang, B.; Zhu, X.; Zhou, Y.; Lu, Z.; Yan, D. *J. Am. Chem. Soc.* **2013**, *135*, 4765−4770.
(20) Zou, J.; Tao, F.; Jiang, M. *Langmuir* **2007**, *23*, 12791−12794.
(21) Nalluri, S. K. M.; Voskuhl, J.; Bultema, J. B.; Boekema, E. J.; Ravoo, B. J. *Angew. Chem., Int. Ed.* **2011**, *50*, 9747−9751.
(22) Yan, Q.; Yuan, J.; Cai, Z.; Xin, Y.; Kang, Y.; Yin, Y. *J. Am. Chem. Soc.* **2010**, *132*, 9268−9270.
(23) Park, C.; Kim, H.; Kim, S.; Kim, C. *J. Am. Chem. Soc.* **2009**, *131*, 16614−16615.
(24) Voskuhl, J.; Stuart, M. C. A.; Ravoo, B. J. *Chem.—Eur. J.* **2010**, *16*, 2790−2796.
(25) Schmidt, B. V. K. J.; Hetzer, M.; Ritter, H.; Barner-Kowollik, C. *Macromolecules* **2013**, *46*, 1054−1065.
(26) Liu, H.; Zhang, Y.; Hu, J.; Li, C.; Liu, S. *Macromol. Chem. Phys.* **2009**, *210*, 2125−2137.
(27) Chen, Y.; Pang, X.-H.; Dong, C.-M. *Adv. Funct. Mater.* **2010**, *20*, 579−586.
(28) Choi, H. S.; Ooya, T.; Huh, K. M.; Yui, N. *Biomacromolecules* **2005**, *6*, 1200−1204.
(29) Sun, G. B.; Wu, D. C.; Liu, Y.; He, C. B.; Chung, T. S.; Goh, S. H. *Polymer* **2005**, *46*, 3355−3362.
(30) Zheng, Y.; Hashidzume, A.; Harada, A. *Macromol. Rapid Commun.* **2013**, *34*, 1062−1066.
(31) Leung, K. C.-F.; Chak, C.-P.; Lo, C.-M.; Wong, W.-Y.; Xuan, S.; Cheng, C. H. K. *Chem.—Asian J.* **2009**, *4*, 364−381.
(32) Ooya, T.; Ito, A.; Yui, N. *Macromol. Biosci.* **2005**, *5*, 379−383.
(33) Tamura, A.; Yui, N. *J. Mater. Chem. B* **2013**, *1*, 3535−3544.
(34) Li, C.; Luo, G.-F.; Wang, H.-Y.; Zhang, J.; Gong, Y.-H.; Cheng, S.-X.; Zhuo, R.-X.; Zhang, X.-Z. *J. Phys. Chem. C* **2011**, *115*, 17651−17659.
(35) Abuchowski, A.; Vanes, T.; Palczuk, N. C.; Davis, F. F. *J. Biol. Chem.* **1977**, *252*, 3578−3581.
(36) Klibanov, A. L.; Maruyama, K.; Torchilin, V. P.; Huang, L. *FEBS Lett.* **1990**, *268*, 235−237.
(37) Ogris, M.; Brunner, S.; Schuller, S.; Kircheis, R.; Wagner, E. *Gene Ther.* **1999**, *6*, 595−605.
(38) Gref, R.; Minamitake, Y.; Peracchia, M. T.; Trubetskoy, V.; Torchilin, V.; Langer, R. *Science* **1994**, *263*, 1600−1603.
(39) Veronese, F. M.; Pasut, G. *Drug Discovery Today* **2005**, *10*, 1451−1458.
(40) Alexis, F.; Pridgen, E.; Molnar, L. K.; Farokhzad, O. C. *Mol. Pharmaceutics* **2008**, *5*, 505−515.
(41) Li, S.-D.; Huang, L. *J. Controlled Release* **2010**, *145*, 178−181.
(42) Rabanel, J.-M.; Hildgen, P.; Banquy, X. *J. Controlled Release* **2014**, *185*, 71−87.
(43) Romberg, B.; Hennink, W. E.; Storm, G. *Pharm. Res.* **2008**, *25*, 55−71.
(44) Gullotti, E.; Yeo, Y. *Mol. Pharmaceutics* **2009**, *6*, 1041−1051.
(45) Du, J.-Z.; Mao, C.-Q.; Yuan, Y.-Y.; Yang, X.-Z.; Wang, J. *Biotechnol. Adv.* **2014**, *32*, 789−803.
(46) Oishi, M.; Sasaki, S.; Nagasaki, Y.; Kataoka, K. *Biomacromolecules* **2003**, *4*, 1426−1432.
(47) Lin, S.; Du, F. S.; Wang, Y.; Ji, S. P.; Liang, D. H.; Yu, L.; Li, Z. C. *Biomacromolecules* **2008**, *9*, 109−115.
(48) Walker, G. F.; Fella, C.; Pelisek, J.; Fahrmeir, J.; Boeckle, S.; Ogris, M.; Wagner, E. *Mol. Ther.* **2005**, *11*, 418−425.
(49) Oupicky, D.; Parker, A. L.; Seymour, L. W. *J. Am. Chem. Soc.* **2002**, *124*, 8−9.
(50) Oishi, M.; Hayama, T.; Akiyama, Y.; Takae, S.; Harada, A.; Yarnasaki, Y.; Nagatsugi, F.; Sasaki, S.; Nagasaki, Y.; Kataoka, K. *Biomacromolecules* **2005**, *6*, 2449−2454.
(51) Zhong, Y.; Yang, W.; Sun, H.; Cheng, R.; Meng, F.; Deng, C.; Zhong, Z. *Biomacromolecules* **2013**, *14*, 3723−3730.
(52) Hatakeyama, H.; Akita, H.; Kogure, K.; Oishi, M.; Nagasaki, Y.; Kihira, Y.; Ueno, M.; Kobayashi, H.; Kikuchi, H.; Harashima, H. *Gene Ther.* **2007**, *14*, 68−77.
(53) Rao, J.; Khan, A. *J. Am. Chem. Soc.* **2013**, *135*, 14056−14059.
(54) Govan, J. M.; McIver, A. L.; Deiters, A. *Bioconjugate Chem.* **2011**, *22*, 2136−2142.
(55) Li, L.; Lv, A.; Deng, X.-X.; Du, F.-S.; Li, Z.-C. *Chem. Commun.* **2013**, *49*, 8549−8551.
(56) Salcher, E. E.; Wagner, E. *Top Curr. Chem.* **2010**, *296*, 227−249.
(57) Cheng, R.; Meng, F.; Deng, C.; Klok, H.-A.; Zhong, Z. *Biomaterials* **2013**, *34*, 3647−3657.
(58) Du, J. Z.; Du, X. J.; Mao, C. Q.; Wang, J. *J. Am. Chem. Soc.* **2011**, *133*, 17560−17563.
(59) Gao, W.; Chan, J. M.; Farokhzad, O. C. *Mol. Pharmaceutics* **2010**, *7*, 1913−1920.
(60) Binauld, S.; Stenzel, M. H. *Chem. Commun.* **2013**, *49*, 2082−2102.
(61) Cheng, J.; Ji, R.; Gao, S.-J.; Du, F.-S.; Li, Z.-C. *Biomacromolecules* **2012**, *13*, 173−179.
(62) Crivello, J. V.; Malik, R.; Lai, Y. L. *J. Polym. Sci., Part A: Polym. Chem.* **1996**, *34*, 3091−3102.
(63) Song, C.-C.; Su, C.-C.; Cheng, J.; Du, F.-S.; Liang, D.-H.; Li, Z.-C. *Macromolecules* **2013**, *46*, 1093−1100.
(64) Qiao, Z.-Y.; Cheng, J.; Ji, R.; Du, F.-S.; Liang, D.-H.; Ji, S.-P.; Li, Z.-C. *RSC Adv.* **2013**, *3*, 24345−24353.
(65) McElvain, S. M. *Chem. Rev.* **1949**, *45*, 453−492.
(66) Khan, A. R.; Forgo, P.; Stine, K. J.; D'Souza, V. T. *Chem. Rev.* **1998**, *98*, 1977−1996.
(67) Schonbeck, C.; Westh, P.; Madsen, J. C.; Larsen, K. L.; Stade, L. W.; Holm, R. *Langmuir* **2010**, *26*, 17949−17957.
(68) Connors, K. A. *Chem. Rev.* **1997**, *97*, 1325−1357.
(69) Schneider, H.-J. *Angew. Chem., Int. Ed.* **2009**, *48*, 3924−3977.
(70) Ng, S. Y.; Shen, H. R.; Lopez, E.; Zherebin, Y.; Barr, J.; Schacht, E.; Heller, J. *J. Controlled Release* **2000**, *65*, 367−374.
(71) Song, C.-C.; Ji, R.; Du, F.-S.; Liang, D.-H.; Li, Z.-C. *ACS Macro Lett.* **2013**, *2*, 273−277.